

1 **Kinetico-Mechanistic Studies on Intramolecular C–X**  
2 **Bond Activation (X = Br, Cl) of Amino-Imino Ligands on**  
3 **Pt(II) Compounds. Prevalence of a Concerted**  
4 **Mechanism in Nonpolar, Polar, and Ionic Liquid Media**

5  
6 Teresa Calvet,<sup>†</sup> Margarita Crespo,<sup>\*,‡</sup> Mercè Font-Bardía,<sup>†</sup> Susanna Jansat,<sup>‡</sup>  
7 and Manuel Martínez<sup>\*,‡</sup>

8

9

10

11

12

13

14 <sup>†</sup> Departament de Mineralogia, Cristal·lografia i Dipòsits Minerals, Universitat de  
15 Barcelona, Martí i Franquès s/n, E-08028 Barcelona, Spain

16 <sup>‡</sup> Departament de Química Inorgànica, Facultat de Química, Universitat de Barcelona,  
17 Martí i Franquès 1-11, E-08028 Barcelona, Spain

18

19 **Abstract**

20           The C–Br and C–Cl oxidative addition reactions of molecules containing a set of  
21 {N-amino,N-imino} chelating donor groups (2-X,6-YC<sub>6</sub>H<sub>4</sub>CHNCH<sub>2</sub>CH<sub>2</sub>NMe<sub>2</sub>, X = Br, Cl;  
22 Y = Cl, H) attached to a {Pt<sup>II</sup>(Ar)<sub>2</sub>} (Ar = Ph, 4-MeC<sub>6</sub>H<sub>4</sub>) have been studied. The Pt(IV)  
23 complexes formed, [PtAr<sub>2</sub>X{2-YCC<sub>5</sub>H<sub>3</sub>CH=NCH<sub>2</sub>CH<sub>2</sub>NMe<sub>2</sub>}], containing a metalated  
24 tridentate [C,N,N'] ligand have been fully characterized by the usual techniques, and the X-  
25 ray crystal structure of the complex with Ar = 4-MeC<sub>6</sub>H<sub>4</sub> and X =Y = Cl has been  
26 determined. Monitoring of the reactions at varying temperatures and pressures and in  
27 different solvents agrees with a mechanism that involves the preliminary decoordination of  
28 the N-amino donor from the ligand to produce a threecoordinated intermediate. This evolves,  
29 via a concerted C–X bond activation, to form a second pentacoordinated intermediate  
30 species that, on coordination of the N-amino donor, produces the final complex. The  
31 kinetic-mechanistic parameters measured indicate that the concerted character of the  
32 process is maintained from nonpolar (xylene and toluene) to polar (acetone) and ionic liquid  
33 ((Bmin(NTf<sub>2</sub>)) media. Furthermore, the  $\Delta V^\ddagger$  values measured indicate that, for the (2,6-  
34 Cl)C<sub>6</sub>H<sub>3</sub>CH=NCH<sub>2</sub>CH<sub>2</sub>NMe<sub>2</sub> ligand, the existence of hydrogen bonding within the  
35 metalating molecule is a determinant for the acceleration observed.

36

37

38

39

40

41

## 42 1. INTRODUCTION

43 The oxidative addition of carbon–halogen bonds is a key step in many stoichiometric  
44 and catalytic reactions mediated by transition-metal complexes.<sup>1</sup> In particular, there is an  
45 increasing evidence of the involvement of palladium(IV) compounds in palladium-catalyzed  
46 processes.<sup>2,3</sup> Due to the comparatively easier access to platinum(IV) species, mechanistic  
47 studies of oxidative addition are often based on organoplatinum chemistry,<sup>4</sup> and these  
48 reactions are well-established.<sup>5</sup> Some studies carried out on intermolecular systems  
49 involving oxidative addition of R<sub>alkyl</sub>X have been conducted for some time and the classical  
50 SN2 mechanism fully established from a kinetic-mechanistic perspective.<sup>6–9</sup> Even ionic  
51 liquid solvent systems have been recently used in order to reveal the importance of polarity  
52 in the reaction medium.<sup>10</sup> For processes involving R<sub>aryl</sub>X oxidative addition reactions, such  
53 a mechanism is prohibitive for an sp<sup>2</sup> carbon center, and a concerted alternative should be  
54 operative.<sup>11</sup> Furthermore, if this process occurs on a previously coordinated organic ligand  
55 (i.e., directing group), a formal intramolecular cyclometallation process will be occurring,  
56 which is expected to require lower energetic demands and produce higher yields.

57 In this respect, intramolecular C<sub>aryl</sub>–X bond activation (X = H, F, Cl, Br) at  
58 dimethylplatinum(II) centers takes place under rather mild conditions for adequately  
59 designed ligands having N donors as directing groups.<sup>12–16</sup> The corresponding  
60 kineticomechanistic study has been also conducted for both ligands containing either one  
61 (imino) or two (amino-imino) nitrogen donor directing groups.<sup>17–20</sup> In recent years, renewed  
62 interest for analogous reactions at diarylplatinum(II) relies on the fact that the resulting  
63 platinum(IV) species are involved in C–C coupling reactions, leading to biphenyl systems  
64 along with formation of several types of platinum(II) compounds containing five-, six-, or  
65 seven-membered platinacycles.<sup>20–24</sup> However, mechanistic studies carried out for this type  
66 of systems are scarce.<sup>25</sup>

67 In this paper, we present a detailed kinetic-mechanistic study on the C–Br and C–Cl  
68 oxidative addition reactions of molecules containing a set of {N-amino, N-imino} chelating

69 donor groups (2-X,6-YC<sub>6</sub>H<sub>4</sub>CHNCH<sub>2</sub>CH<sub>2</sub>NMe<sub>2</sub>, X = Br, Cl; Y = Cl, H) attached to a  
70 {Pt<sup>II</sup>(Ar)<sub>2</sub>} (Ar = Ph, 4-MeC<sub>6</sub>H<sub>4</sub>) unit.

71 The Pt(IV) complexes formed, [PtAr<sub>2</sub>X{2-YCC<sub>5</sub>H<sub>3</sub>CH=NCH<sub>2</sub>CH<sub>2</sub>NMe<sub>2</sub>}],  
72 containing a metalated tridentate [C,N,N'] ligand, have been fully characterized by the usual  
73 techniques, indicating the existence of the fac-[C,N,N'] arrangement together with the usual  
74 mer-[C,N,N'] isomer in some cases. The X-ray crystal structure of the complex with Ar = 4-  
75 MeC<sub>6</sub>H<sub>4</sub> and X = Y = Cl has also been determined, agreeing with the characterization data  
76 in solution. The kineticomechanistic results agree with the concerted mechanism established  
77 for previous studies on monodentate N-imino directing group systems. The absence of any  
78 polar component in the concerted transition state proposed is made clear by the independence  
79 of the parameters measured for ortho-xylene, toluene, acetone, or (Bmin)(NTf<sub>2</sub>) (1-butyl-3-  
80 methylimidazolium bis{trifluoromethanesulfonyl}imide) solvents. Furthermore, the  
81 continuity of the mechanism proposed is made clear by a very good alignment with the  
82  $\Delta H^\ddagger/\Delta S^\ddagger$  compensation plot for all the systems available in the literature.<sup>19</sup> The more  
83 positive values found for the systems studied agree with the need of the N-amino  
84 decoordination as a preliminary steady-state step to the proper C-X bond activation, as  
85 already found for equivalent {N-amino,N-imino} chelating systems with {Pt<sup>II</sup>(Me)<sub>2</sub>}  
86 units.<sup>12</sup> The existence of hydrogen-bonding interactions involved in the reactivity of the 2,6-  
87 Cl<sub>2</sub>C<sub>6</sub>H<sub>4</sub>CHNCH<sub>2</sub>CH<sub>2</sub>NMe<sub>2</sub> ligand is also made evident by the usual lack of parallelism in  
88 the  $\Delta V^\ddagger/\Delta S^\ddagger$  trend.<sup>19,26</sup>

89

90

91

92

## 93 2. RESULTS AND DISCUSSION

94           **Compounds.** The syntheses of Pt(IV) compounds [PtAr<sub>2</sub>X {2-YCC<sub>5</sub>H<sub>3</sub>CH =  
95 NCH<sub>2</sub>CH<sub>2</sub>NMe<sub>2</sub>}] (Ar = Ph or 4-MeC<sub>6</sub>H<sub>4</sub>; X = Br or Cl; Y = Cl or H) have been previously  
96 reported.<sup>20,24</sup> These compounds are formed via the intramolecular oxidative addition of  
97 C–X bonds from the corresponding Pt(II) coordination compounds [PtAr<sub>2</sub>{2-X,6-  
98 YC<sub>6</sub>H<sub>3</sub>CH = NCH<sub>2</sub>CH<sub>2</sub>NMe<sub>2</sub>}] . Compound [Pt{4-MeC<sub>6</sub>H<sub>4</sub>} 2Cl {2-ClCC<sub>5</sub>H<sub>3</sub>CH =  
99 NCH<sub>2</sub>CH<sub>2</sub>NMe<sub>2</sub>}] (**3-Cl,Cl**) was characterized crystallographically in this work. The  
100 structure depicted in Figure 1 shows the three carbon donors in the usual *fac*-PtC<sub>3</sub> geometry  
101 and the tridentate ligand adopting a *mer*-[C,N,N'] disposition, in agreement with the  
102 arrangement reported for [PtMe<sub>2</sub>Cl {2-ClCC<sub>5</sub>H<sub>3</sub>CH = NCH<sub>2</sub>CH<sub>2</sub>NMe<sub>2</sub>}] .<sup>12</sup> The Pt–NMe<sub>2</sub>  
103 distance, 2.298(4) Å, is significantly longer than that for the Pt–NCH bond, 2.059(3) Å,  
104 which is consistent with the relatively weak ligand character of tertiary amines for  
105 platinum.<sup>27</sup> All bond distances are in the expected range, and the bond angles at the platinum  
106 center deviate slightly from the ideal 90°. The smallest, N1–Pt–N2 = 79.72 (12)° and  
107 C1–Pt–N2 = 81.03 (14)°, involve the tridentate [C,N,N'] ligand. The <sup>1</sup>H NMR spectra of  
108 compounds [Pt{4-MeC<sub>6</sub>H<sub>4</sub>} 2Cl {2-ClCC<sub>5</sub>H<sub>3</sub>CH = NCH<sub>2</sub>CH<sub>2</sub>NMe<sub>2</sub>}] (**3-Cl,Cl**) and  
109 [Pt{4-MeC<sub>6</sub>H<sub>4</sub>} 2Cl - {CC<sub>5</sub>H<sub>4</sub>CH = NCH<sub>2</sub>CH<sub>2</sub>NMe<sub>2</sub>}] (**3-Cl,H**) in CDCl<sub>3</sub> or acetone-d<sub>6</sub>  
110 indicate the presence of a single isomer, and the structure determined in the X-ray study of  
111 **3-Cl,Cl** is assumed. As previously reported,<sup>24</sup> these compounds react in solution to give  
112 seven-membered metallacycles and toluene, which prevents further studies.

113           In this respect, the higher inertness of compound [Pt {4-MeC<sub>6</sub>H<sub>4</sub>} 2Br {CC<sub>5</sub>H<sub>4</sub>CH  
114 = NCH<sub>2</sub>CH<sub>2</sub>NMe<sub>2</sub>}] (**3-Br,H**) allows for a more detailed study of its behavior in different  
115 deuterated solvents. Analysis of the signals in the –N = CH– region indicates the presence  
116 of a single isomer in deuterated toluene, while two isomers are observed in CDCl<sub>3</sub> and  
117 CD<sub>3</sub>COCD<sub>3</sub> (relative ratios of 91:9 and 89:11, respectively); in dmsO-d<sub>6</sub>, three resonances  
118 are apparent with relative ratios of 3:94:3. Considering that the three Pt–C bonds of the **3-  
119 Br,H** compound have to be mutually *fac*, due to the donor character of the ligands around

120 the platinum center,<sup>28,29</sup> two different isomers with the [C,N,N'] ligand either in *mer* or *fac*  
121 arrangements can exist in solution (Scheme 1).

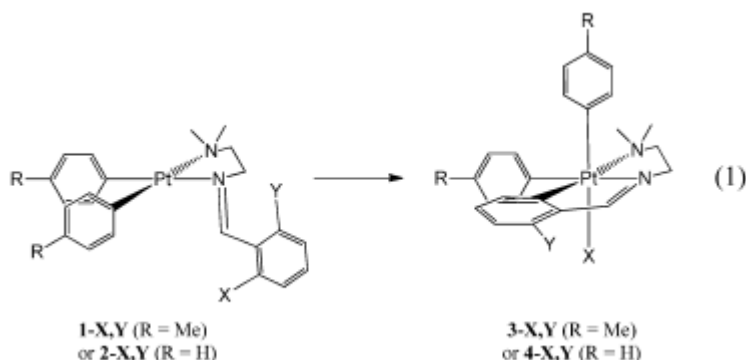
122 Calculations carried out for analogous [PtMe<sub>2</sub>X (C,N,N')] compounds indicated a  
123 slightly higher stability for the *mer*-versus *fac*-[C,N,N'] ligand arrangement (ca. 8–9  
124 kcal/mol), as expected due to the preference of the metalated imine ligand to be  
125 approximately planar.<sup>12</sup> The *mer*-[C,N,N'] structure is thus assigned to the major isomer of  
126 **3-Br,H** observed in CDCl<sub>3</sub> based on the NOESY cross-peaks between the tolyl groups and  
127 both methyl substituents from the amino group. Although the trend in chemical shifts, in  
128 particular, for the iminic hydrogen, observed for the major isomer (Table 1) can be fitted to  
129 the different polarity parameters of the different solvents used in a reasonable way, NOESY  
130 spectra indicated that a different arrangement of the [C,N,N'] unit might occur in some of  
131 the media. In this respect, the NOESY contact between the ortho proton signals of the  
132 metalated ring and both dimethylamino groups, observed for the major isomer in dmsO,  
133 points to the alternative facial arrangement of the [C,N,N'] ligand in this solvent.  
134 Nevertheless, an easy isomerization between the *mer* and the *fac* arrangement of the [C,N,N']  
135 ligand is expected from the quasi-labile character of these compounds, as already established  
136 for the substitution of the SMe<sub>2</sub> ligand in similar [C,N] cyclometalated Pt(IV) complexes.<sup>30</sup>  
137 Furthermore, the coexistence of the two isomers indicated in Scheme 1 has already been  
138 established in other systems of the same family, as well as their interconversion on changing  
139 the size of the ancillary neutral ligand from SMe<sub>2</sub> to PPh<sub>3</sub>.<sup>31</sup> Finally, decoordination of the  
140 dimethylamino moiety in dmsO might account for the observation of a third imine resonance  
141 in this solvent. Because of the small intensity of the signal observed, any further assignment  
142 to a specific isomer has not been conducted.

143 Interestingly, the signals corresponding to the ethylene bridge protons (= N – CH<sub>2</sub> –  
144 CH<sub>2</sub> – N (CH<sub>3</sub>)<sub>2</sub>) of the [C,N,N'] metalated ligand show diverse patterns appearing at very  
145 different chemical shifts, depending on the solvents used. Even in dmsO and toluene solution,  
146 the four protons appear as nonequivalent. In the latter solvent, they appear in the widest  
147 range (4.12, 3.35, 3.17, and 1.87 ppm) with a marked upfield chemical shift for one of the  
148 –CH<sub>2</sub>–CH<sub>2</sub>–N(CH<sub>3</sub>)<sub>2</sub> nuclei. These data cannot be rationalized on the exclusive basis of the

149 different polarities of the solvents and can be related to different conformations of the [N,N']  
150 chelate as well as different preferred orientations of the tolyl ligands.

151 **Kinetic-Mechanistic Studies.** The oxidative addition reaction of the C–X bond  
152 occurring on **1 - Cl, H**, **2 – Cl, H**, **1 - Br, H**, and **1 – Cl, Cl** Pt (II) complexes (Scheme 2),  
153 producing the corresponding Pt(IV) derivatives (eq 1), has been timeresolved by monitoring  
154 the changes in the UV–vis and proton NMR spectra of the samples in different solvents.

155 Proton NMR spectra monitoring of the reactions carried out in toluene, after reduced  
156 pressure evaporation of the solvent, indicated that, effectively, the process followed  
157 corresponds to the reaction shown in eq 1 on the time scale used. Thus, the validity of the  
158 UV–vis monitoring of the reaction under the same conditions has been proved. In all cases,  
159 a very wellbehaved first-order behavior has been observed with a large decrease of the  
160 absorbance in the electronic spectrum at ca. 400 nm, which corresponds to the disappearance  
161 of the Pt(II) complex.<sup>17,32</sup> When the compounds were left for longer times in the reaction  
162 medium, a new increase of the response of the electronic spectra at this wavelength was  
163 observed, corresponding to the formation of new Pt(II) species.<sup>22,25</sup> These reductive  
164 elimination processes are currently under study. Specifically, the isolation of neat **1-Br,H**  
165 has not been achieved; nevertheless, as stated above, NMR monitoring indicates that the  
166 kinetic profiles measured effectively correspond to the C–Br bond activation on compound  
167 **1-Br,H**.



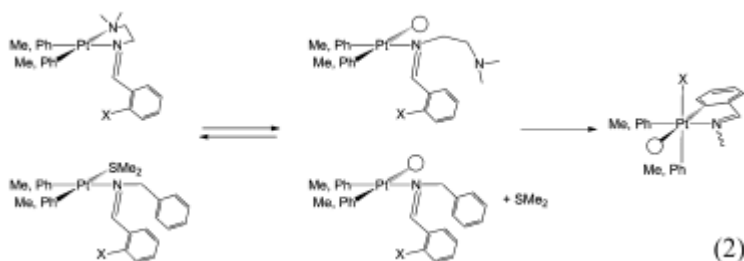
170 The reactions were followed in toluene, ortho-xylene, (Bmin)(NTf<sub>2</sub>), and acetone  
171 solutions at different concentrations, temperatures, and pressures via conventional electronic  
172 spectroscopy and using the convenient instrumentation indicated in the Experimental  
Section. Changes in the concentration of the platinum complex within the  $(0.5\text{--}5) \times 10^{-4}$  M

margin produced no changes in the measured rate constants, as expected for reactions as those indicated in eq 1. Similarly, the use of the diversity of solvents indicated in the processes does not produce significant changes in the reaction rates, as already found for the concerted oxidative addition occurring on very similar complexes (Figure 2).<sup>17,18</sup> This is specially relevant for the use of (Bmin)(NTf<sub>2</sub>) ionic liquid as the solvent, given the fact that the use of such a solvent has been found having determinant effects when changes in the polarity on going to the transition state are involved.<sup>10,33,34</sup>

Table 2 collects the relevant kinetic and activation parameters measured for the reactions monitored. From the data, it is clear that rather different values have been determined for the two sets of compounds studied: (i) those having a monodentate {N-imino} metalating and an ancillary dimethylsulfide ligand and (ii) those with an {N-imino,N-amino} bidentate unit. For the former, the reaction occurs in a facile way at room temperature with little enthalpic requirements and a high degree of ordering and compression on going to the transition state. In this case, the reaction sequence had been established as one that involves the sulfide ligand dissociation, formation of an undetected 14-electron intermediate, and a subsequent facile concerted C–X bond activation.<sup>17,35,36</sup> Accordingly, if, for the {N-imino,N-amino} bidentate systems, such a 14-electron intermediate is responsible for the C–X bond activation, its energetic demands should be much higher,<sup>37</sup> which is effectively seen in the activation parameters. Furthermore, in this case, the dangling arrangement of the Namino moiety should also produce a definite increase of the volume and entropy of activation, despite keeping the concerted nature of the C–X bond oxidative addition. Figure 3 shows a very good  $\Delta H^\ddagger/\Delta S^\ddagger$  compensation plot for all the systems indicated in Table 2, which corroborates the uniformity of the C–X bond activation processes being studied, independent of the nature of the directing groups of the metalating ligand.<sup>38,39</sup> From the data collected, it is also clear that the changes introduced by changing a 4-MeC<sub>6</sub>H<sub>4</sub> for a phenyl spectator ligand do not have any significant effect on the process.

From the data collected in Table 2, it is also clear that the compounds having two methyl ancillary ligands have smaller  $\Delta H^\ddagger$  values, while the  $\Delta S^\ddagger$  values are more negative than for the equivalent bis-aryl analogues (1-Cl,H/v, 1-Br,H/vi, 1 - Cl,Cl/vii, *xiii/xiv*).<sup>22</sup> The

202 effect is specially pronounced for entries *xii* and *xiv*, which are related to monodentate  
 203 dimethylsulfide complexes. The trend can be associated with the lower donor character of  
 204 the phenyl ligands, when compared with the equivalent complex with methyl groups, that  
 205 hampers the relative dissociation of the nonorganometallic ligands and the formation of the  
 206 14-electron intermediate, especially for monodentate dimethylsulfide systems (eq 2).



207

208 A close examination of the data in Table 2 shows, nevertheless, two sets of values  
 209 that fall out of the expected  $\Delta S^\ddagger/\Delta V^\ddagger$  correlation plot indicated in Figure 4 (provided no  
 210 hydrogen bonding is involved in the activation process).<sup>19,22,26,40</sup> For compound  
 211 [PtMe<sub>2</sub>{CC<sub>5</sub>F<sub>5</sub>CHNCH<sub>2</sub>C<sub>6</sub>H<sub>5</sub>}- (SMe<sub>2</sub>)], *ix*, the possible hydrogen bonding has been found  
 212 to favor an earlier transition state for the C–F bond activation and produce such a deviation  
 213 (low enthalpy, very negative entropy, and small contraction).<sup>19</sup> In the present case for  
 214 compound 1 - **Cl,Cl**, this explanation is rather difficult to come to terms with, unless a  
 215 hydrogen bond between the nonmetalating chloride *ortho* substituent in the ring and the =  
 216 CH – hydrogen is claimed, as already established in other similar systems.<sup>37,41</sup> If this is the  
 217 case, a much more ordered transition state can be expected (Scheme 3), thus explaining the  
 218 anomalous  $\Delta S^\ddagger/\Delta V^\ddagger$  correlation point.

219 In this respect, the existence of the hydrogen-bonding interaction indicated in  
 220 Scheme 3, involving a nonmetalating chloride group, can also explain the much less  
 221 favorable enthalpy found for the activation of the C–Cl bond in **1-Cl,H** when compared with  
 222 **1-Cl,Cl**. Furthermore, time-resolved proton NMR monitoring of the reaction from **1-Cl,H**  
 223 to **3- Cl,H** indicated the presence in very small quantities (5–10%) of free toluene and a five-  
 224 membered Pt(II) compound.<sup>42</sup> The latter has been putatively associated with that obtained  
 225 by an *ortho* C–H bond activation of the ligand, from a species, such as that indicated in

226 Scheme 3, involving a three-centered H–Pt–C interaction, followed by tolyl–H reductive  
227 elimination from a hydride Pt(IV) intermediate compound.<sup>22</sup>

228

229

230

231

### 232 3. CONCLUSIONS

233 The oxidative addition reaction of the (2-X,6-Y) C<sub>6</sub>H<sub>3</sub>CH = NCH<sub>2</sub>CH<sub>2</sub>NMe<sub>2</sub> (X =  
234 Br or Cl; Y = H, or Cl) ligands on Pt(II) organometallic compounds has been studied from a  
235 kineticomechanistic perspective. In all cases, the process from [PtAr<sub>2</sub>{(2-X,6-  
236 Y)C<sub>6</sub>H<sub>3</sub>CH=NCH<sub>2</sub>CH<sub>2</sub>NMe<sub>2</sub>}] (Ar = Ph or 4-MeC<sub>6</sub>H<sub>4</sub>) produces the corresponding Pt(IV)  
237 species [PtAr<sub>2</sub>X{2-YCC<sub>5</sub>H<sub>2</sub>CH=NCH<sub>2</sub>CH<sub>2</sub>NMe<sub>2</sub>}]. The monitoring of the reactions at  
238 varying temperatures and pressures and in different solvents indicates a mechanism that  
239 involves the preliminary decoordination of the N-amino donor from the ligand to produce a  
240 three-coordinated intermediate. This evolves, via a concerted C–X bond activation, to form  
241 a second pentacoordinated intermediate species that, on coordination of the N-amino donor,  
242 produces the final complex. The kinetic and activation parameters measured indicate that the  
243 concerted character of the process is maintained from nonpolar (xylene and toluene) to polar  
244 (acetone) and ionic liquid ((Bmin) (NTf<sub>2</sub>)) media and that an excellent thermal activation  
245 parameter compensation plot exists for all studied systems of the same family, which include  
246 reported monodentate imine and ancillary SMe<sub>2</sub> ligands. The expected  $\Delta V^\ddagger/\Delta S^\ddagger$   
247 compensation plot indicates that, for the (2,6-Cl) C<sub>6</sub>H<sub>3</sub>CH = NCH<sub>2</sub>CH<sub>2</sub>NMe<sub>2</sub> ligand, the  
248 existence of hydrogen bonding within the molecule is a determinant for the acceleration  
249 observed, as well as for the unexpected large expansion on going to the transition state. The  
250 same effects had already been observed for other concerted reaction systems prone to  
251 internal hydrogen bonding.

252

253

254

255

256

257

258

259

## 260 4. EXPERIMENTAL SECTION

261 **General.** Microanalyses were performed at the Serveis Científico-Tècnics  
262 (Universitat de Barcelona). Electrospray mass spectra were performed at the Servei  
263 d'Espectrometria de Masses (Universitat de Barcelona) in a LC/MSD-TOF spectrometer  
264 using H<sub>2</sub>O–CH<sub>3</sub>CN (1:1) to introduce the sample. NMR spectra were performed at the  
265 Unitat de RMN d'Alt Camp de la Universitat de Barcelona using Mercury-400 or Varian-  
266 500 spectrometers and referenced to SiMe<sub>4</sub>. Δ values are given in parts per million and J  
267 values in hertz. The following abbreviations are used: s = singlet; d = doublet; t = triplet; m  
268 = multiplet; br = broad. The (Bmim)(NTf<sub>2</sub>) ionic liquid (99.5%) was purchased from  
269 Solvionic and was used without further purification.

270 **Preparation of Compounds.** Compounds *cis*-[Pt{4-MeC<sub>6</sub>H<sub>4</sub>}<sub>2</sub>{μ-SEt<sub>2</sub>}<sub>2</sub>]<sub>2</sub>,<sup>43</sup>  
271 1-Cl,Cl,<sup>24</sup> 2-Cl,H,<sup>20</sup> 3-Br,H,<sup>24</sup> 3-Cl,Cl<sup>24</sup> and 4-Cl,H,<sup>20</sup> as well as the corresponding  
272 ligands,<sup>12</sup> were prepared as reported elsewhere. The detailed preparative procedures and  
273 characterization data are collected in the Supporting Information.

274 **X-ray Structure Analysis.** A prismatic crystal (0.1 × 0.1 × 0.2 mm) was  
275 selected and mounted on a MAR345 diffractometer with an image plate detector. Intensities  
276 were collected with graphite monochromatized Mo Kα radiation. The structure was solved  
277 by direct methods using the SHELXS computer program and refined by the full-matrix least-  
278 squares method, with the method, with the SHELXL97 computer program using 27 210  
279 reflections (very negative intensities were not assumed).<sup>44</sup> The function minimized was  
280  $\Sigma w||F_o|^2 - |F_c|^2|^2$ , where  $w = [\sigma^2(I) + (0.0397 P)^2 + 3.1962 P]^{-1}$  and  $P = (|F_o|^2 + 2|F_c|^2)/3$ .  
281  $f$ ,  $f'$ , and  $f''$  were taken from the *International Tables of Xray Crystallography*.<sup>45</sup> All  
282 hydrogen atoms were computed and refined using a riding model with an isotropic  
283 temperature factor equal to 1.2 times the equivalent temperature factor of the atom to which  
284 they are linked. Further details are given in Table 3.

285 **Kinetics.** The kinetic profiles for the reactions were followed by UV–vis  
286 spectroscopy in the 700–300 nm range. Atmospheric pressure runs were recorded on  
287 HP8453 or Cary50 instruments equipped with thermostatted multicell transports. Observed

288 rate constants were derived from absorbance versus time traces at the wavelengths where a  
289 maximum increase and/or decrease of absorbance was observed. For runs at variable  
290 pressure, a previously described pressurizing system and pill-box cell were used;<sup>46,47</sup> the  
291 system was connected to a J&M TIDAS spectrophotometer that was used for the absorbance  
292 measurements. The calculation of the observed rate constants from the absorbance versus  
293 time monitoring of reactions, studied under second- or first-order concentration conditions,  
294 were carried out using the SPECFIT software.<sup>32</sup> The general kinetic technique is that  
295 previously described.<sup>19,21,48</sup> Table S1 (Supporting Information) collects the obtained  $k_{\text{obs}}$   
296 values for all the systems studied as a function of the starting complex, process studied,  
297 platinum and imine concentrations, pressure, and temperature. All post-run fittings were  
298 carried out by the standard available commercial programs.

299

300

301

302

303

304

305

306

307

308

309

310 **5. ACKNOWLEDGEMENTS**

311 Financial support from projects CTQ2009-14443-C02-02 and CTQ2009-11501 from  
312 the Spanish Ministerio de Ciencia e Innovación is acknowledged

313

314

315

316

317

318 **AUTHOR INFORMATION**

319 **Corresponding Author**

320 \*E-mail: manel.martinez@qi.ub.edu (M.M.), margarita.crespo@qi.ub.edu (M.C.).

321

322

323

324 **Notes**

325 The authors declare no competing financial interest.

326

327

328

329

330

331 **6. REFERENCES**

- 332 (1) Crabtree, R. H. *The Organometallic Chemistry of the Transition Metals*; John Wiley  
333 & Sons: New York, 2005.
- 334 (2) Hickman, A. J.; Sanford, M. S. *Nature* 2012, 484, 177–185.
- 335 (3) Sehnal, P.; Taylor, R. J. K.; Fairlamb, I. J. S. *Chem. Rev.* 2010, 110, 824–889.
- 336 (4) Canty, A. J. *Dalton Trans.* 2009, 10409–10417.
- 337 (5) Rendina, L. M.; Puddephatt, R. J. *Chem. Rev.* 1997, 97, 1735–1754.
- 338 (6) Hoseini, S. J.; Nasrabadi, H.; Nabavizadeh, S. M.; Rashidi, M.; Puddephatt, R. J.  
339 *Organometallics* 2012, 31, 2357–2366.
- 340 (7) Jamali, S.; Nabavizadeh, S. M.; Rashidi, M. *Inorg. Chem.* 2008, 47, 5441–5452.
- 341 (8) Nabavizadeh, S. M.; Hoseini, S. J.; Momeni, B. Z.; Shahabadi, N.; Rashidi, M.;  
342 Pakiari, A. H.; Eskandari, K. *Dalton Trans.* 2008, 2414–2421.
- 343 (9) Nabavizadeh, S. M.; Habibzadeh, S.; Rashidi, M.; Puddephatt, R. J. *Organometallics*  
344 2010, 29, 6359–6368.
- 345 (10) Nabavizadeh, S. M.; Shahsavari, H. R.; Sepehrpour, H.; Hosseini, F. N.; Jamali, S.;  
346 Rashidi, M. *Dalton Trans.* 2010, 39, 7800–7805.
- 347 (11) Jordan, R. B. *Reaction Mechanisms of Inorganic and Organometallic Systems*; Oxford  
348 University Press: New York, 2007.
- 349 (12) Anderson, C. M.; Crespo, M.; Jennings, M. C.; Lough, A. J.; Ferguson, G.; Puddephatt,  
350 R. J. *Organometallics* 1991, 10, 2672–2679.
- 351 (13) Anderson, C. M.; Crespo, M.; Ferguson, G.; Lough, A. J.; Puddephatt, R. J.  
352 *Organometallics* 1992, 11, 1177–1181.
- 353 (14) Crespo, M.; Solans, X.; Font-Bardía, M. *Organometallics* 1995, 14, 355.
- 354 (15) Crespo, M.; Solans, X.; Font-Bardía, M. *J. Organomet. Chem.* 1996, 105–113.
- 355 (16) Anderson, C. M.; Crespo, M.; Font-Bardía, M.; Klein, A.; Solans, X. *J. Organomet.*  
356 *Chem.* 2000, 601, 22–33.
- 357 (17) Crespo, M.; Martínez, M.; Sales, J.; Solans, X.; Font-Bardía, M. *Organometallics*

- 358 1992, 11, 1288–1295.
- 359 (18) Crespo, M.; Martínez, M.; Sales, J. *Organometallics* 1993, 12, 4297–4304.
- 360 (19) Crespo, M.; Martínez, M.; de Pablo, E. J. *Chem. Soc., Dalton Trans.* 1997, 1231–1235.
- 361 (20) Crespo, M.; Font-Bardia, M.; Solans, X. *Organometallics* 2004, 23, 1708–1713.
- 362 (21) Font-Bardia, M.; Gallego, C.; Martínez, M.; Solans, X. *Organometallics* 2002, 21,  
363 3305–3307.
- 364 (22) Calvet, T.; Crespo, M.; Font-Bardía, M.; Gómez, K.; González, G.; Martínez, M.  
365 *Organometallics* 2009, 28, 5096–5106.
- 366 (23) Crespo, M.; Font-Bardia, M.; Calvet, T. *Dalton Trans.* 2011, 40, 9431–9438.
- 367 (24) Martín, R.; Crespo, M.; Font-Bardia, M.; Calvet, T. *Organometallics* 2009, 28,  
368 587–597.
- 369 (25) Gallego, C.; Martínez, M.; Safont, V. S. *Organometallics* 2007, 26, 527–537.
- 370 (26) Gallego, C.; González, G.; Martínez, M.; Merbach, A. E. *Organometallics* 2004, 23,  
371 2434–2438.
- 372 (27) Esteban, J.; Font-Bardia, M.; Gallego, C.; González, G.; Martínez, M.; Solans, X.  
373 *Inorg. Chim. Acta* 2003, 351, 269–277.
- 374 (28) Scott, J. D.; Puddephatt, R. J. *Organometallics* 1986, 5, 1538–1544.
- 375 (29) Canty, A. J.; Patel, J.; Rodemann, T.; Ryan, J. H.; Skelton, B. W.; White, A. H.  
376 *Organometallics* 2004, 23, 3466–3473.
- 377 (30) Bernhardt, P. V.; Gallego, C.; Martínez, M. *Organometallics* 2000, 19, 4862–4869.
- 378 (31) Font-Bardía, M.; Gallego, C.; González, G.; Martínez, M.; Merbach, A. E.; Solans, X.  
379 *Dalton Trans.* 2003, 1106–1113.
- 380 (32) Binstead, R. A.; Zuberbuhler, A. D.; Jung, B. SPECFIT32. [3.0.34]; Spectrum  
381 Software Associates: Marlborough, MA, 2005.
- 382 (33) Aviles, T.; Jansat, S.; Martínez, M.; Montilla, F.; Rodríguez, C. *Organometallics* 2011,  
383 30, 3919–3922.
- 384 (34) Schmeisser, M.; Heinemann, F. W.; Illner, P.; Puchta, R.; Zahl, A.; van Eldik, R. *Inorg.*

- 385 Chem. 2011, 50, 6685–6695.
- 386 (35) Rashidi, M.; Fakhroeiian, Z.; Puddephatt, R. J. J. Organomet. Chem. 1991, 406,  
387 261–267.
- 388 (36) Scott, J. D.; Puddephatt, R. J. Organometallics 1983, 2, 1643–1648.
- 389 (37) Crespo, M.; Font-Bardía, M.; Granell, J.; Martínez, M.; Solans, X. Dalton Trans. 2003,  
390 3763–3769.
- 391 (38) Tobe, M. L.; Burgess, J. Inorganic Reaction Mechanisms; Longman: Harlow, Essex,  
392 U.K., 1999.
- 393 (39) Wilkins, R. G. Kinetics and Mechanisms of Reactions of Transition Metal Complexes;  
394 VCH: New York, 1991.
- 395 (40) Bernhardt, P. V.; Bozoglian, F.; Macpherson, B. P.; Martínez, M.; Merbach, A. E.;  
396 González, G.; Sienna, B. Inorg. Chem. 2004, 43, 7187–7195.
- 397 (41) Crespo, M.; Granell, J.; Solans, X.; Font-Bardía, M. Organometallics 2002, 21,  
398 5140–5143.
- 399 (42) <sup>1</sup>H NMR data (CDCl<sub>3</sub>, 400 MHz,  $\delta$  in ppm,  $J$  in Hz) assigned to the five-membered  
400 cyclometalated platinum(II) compound [Pt (4 - MeC<sub>6</sub>H<sub>4</sub>) {2 -  
401 ClCC<sub>5</sub>H<sub>3</sub>CHNCH<sub>2</sub>CH<sub>2</sub>NMe<sub>2</sub>}]: 8.77 [s,  $J$ (H–Pt) = 48, 1H, CHN], 4.07 [td,  $J$ (H–H)  
402 = 6.0; 1.6, 2H, CH<sub>2</sub>], 3.98 [td,  $J$ (H–H) = 6.0; 1.2, 2H, CH<sub>2</sub>], 2.88 [s, 6H, N(CH<sub>3</sub>)<sub>2</sub>].
- 403 (43) Steele, B. R.; Vrieze, K. Trans. Met. Chem. 1977, 2, 169–174.
- 404 (44) Sheldrick, G. M. SHELX97: Programs for Crystal Structure Analysis (Release 97-2);  
405 Universität Göttingen: Göttingen, Germany, 1998.
- 406 (45) International Tables for X-Ray Crystallography; Kynoch Press: Birmingham, U.K.,  
407 1974; Vol. IV, pp 99–100, 149.
- 408 (46) Gómez, M.; Granell, J.; Martínez, M. Organometallics 1997, 16, 2539–2546.
- 409 (47) van Eldik, R., Ed. Inorganic High Pressure Chemistry; Elsevier: Amsterdam, 1986; pp  
410 1–68.
- 411 (48) Roiban, G. D.; Serrano, E.; Soler, T.; Aullón, G.; Grosu, I.; Cativiela, C.; Martínez,

412 M.; Urriolabeitia, E. P. *Inorg. Chem.* 2011, 50, 8132–8143.

413

414

415

416

417

418

419

420

421

422

423

424

425

426

427 **Table 1** Selected NMR Data in Several Deuterated Solvents<sup>a</sup>

428

solvent	$\delta$ (-N= <u>CH</u> -)	$\delta$ (-N( <u>CH</u> <sub>3</sub> ) <sub>2</sub> )	$\delta$ (+ <u>CH</u> <sub>3</sub> -C <sub>6</sub> H <sub>4</sub> -)
dmsob <sup>b</sup>	8.91 (45)	2.74 (-)	2.25
acetone <sup>H</sup>	8.87 (47)	2.48 (-)	2.04
		2.59 (17)	2.07
CDCl <sub>3</sub> <sup>b</sup>	8.58 (45)	2.97 (10)	2.34
		2.46 (15)	2.14
toluene	7.28 (45)	2.64 (10)	2.34
		1.95 (15)	2.00

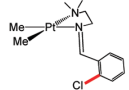
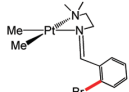
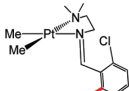
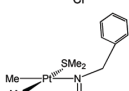
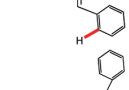
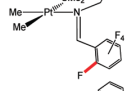
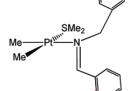
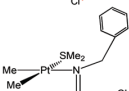
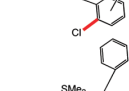
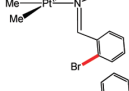
<sup>a</sup>Chemical shifts in ppm and coupling constants  $J(\text{Pt-H})$  in Hz in parentheses. <sup>b</sup>Data for the major isomer.

429

430

431

432 **Table 2.** Kinetic and Activation Parameters for the Oxidative Addition of C–X Bonds on  
 433 the Platinum(II) Complexes Indicated in Scheme 2 in Toluene Solution. Relevant Values in  
 434 Acetone Solution for Similar Compounds Are Also Included

Entry	Complex	Reference	$10^5 \times {}^{298}k / \text{s}^{-1}$	$\Delta H^\ddagger / \text{kJ mol}^{-1}$	$\Delta S^\ddagger / \text{J K}^{-1} \text{mol}^{-1}$	$\Delta V^\ddagger / \text{cm}^3 \text{mol}^{-1}$	
435	<b>i</b>	<b>1-Cl,H</b>	This work	0.13 <sup>a</sup>	127±6	66±17	9±2
436	<b>ii</b>	<b>2-Cl,H</b>	This work	0.065 <sup>a</sup>	124±5	50±15	Not determined
437	<b>iii</b>	<b>1-Br,H</b>	This work	31 <sup>a</sup>	100±4	21±13	10±1
438	<b>iv</b>	<b>1-Cl,Cl</b>	This work	13 <sup>a</sup>	87±2	-30±7	16±1
439	<b>v</b>		12	5.5	101±5	10±17	Not determined
440	<b>vi</b>		12	31	97±2	11±10	Not determined
441	<b>vii</b>		12	65	71±7	-70±25	Not determined
442	<b>viii</b>		17,19	340	60±5	-100±10	-17±1
443	<b>ix</b>		18,19	340	30±5	-195±15	-14±1
444	<b>x</b>		17,19	210	60±9	-93±28	-20±1
445	<b>xi</b>		19	540	70±5	-70±5	-12±1
446	<b>xii</b>		17,19	590	48±7	-125±23	-22±1
447	<b>xiii</b>		17,19	260	23±1	-218±2	-31±1
448	<b>xiv</b>		22	140	87±4	-11±13	-4±1

455 <sup>a</sup> Extrapolated from the thermal parameters indicated.

456

457

458 **Table 3** Crystallographic and Refinement Data

459

formula	$C_{25}H_{28}Cl_2N_2Pt \cdot CH_2Cl_2$
fw	707.41
temp, K	293(2)
wavelength, Å	0.71073
cryst syst	monoclinic
space group	$P2_1/c$
<i>a</i> , Å	13.277(4)
<i>b</i> , Å	13.065(3)
<i>c</i> , Å	20.035(5)
$\alpha$ , deg	90
$\beta$ , deg	128.322(17)
$\gamma$ , deg	90
<i>V</i> , Å <sup>3</sup> ; <i>Z</i>	2726.5(12); 4
<i>d</i> (calcd), Mg/m <sup>3</sup>	1.723
abs coeff, mm <sup>-1</sup>	5.556
<i>F</i> (000)	1384
rfns coll./unique	27210/8164 [ <i>R</i> (int) = 0.0645]
data/restraint/parameters	8164/8/330
GOF on <i>F</i> <sup>2</sup>	1.068
final <i>R</i> <sub>1</sub> ( <i>I</i> > 2σ( <i>I</i> )); w <i>R</i> <sub>2</sub>	0.0330; 0.0903
<i>R</i> (all data); w <i>R</i> <sub>2</sub>	0.0359; 0.0939
peak and hole, e·Å <sup>-3</sup>	1.987 and -1.315

460

461

462

463

464 **Figures Captions**

465 **Figure 1.** Molecular structure of compound 3-Cl,Cl. Selected bond lengths (Å) and angles  
466 (deg) with estimated standard deviations: Pt1-C1 = 2.004(4), Pt1-C12 = 2.036(4), Pt1-C19  
467 = 2.026(4), Pt1-N1 = 2.298(4), Pt1-N2 = 2.059(3), Pt1-Cl1 = 2.4681(10); C1-Pt1-Cl1 =  
468 89.72(11), C1-Pt1-C12 = 84.30(15), C1-Pt1-C19 = 98.63(16), C1-Pt1-N2 = 81.03(14),  
469 C12-Pt1-N1 = 98.84(14), C12-Pt1-N2 = 93.93(15), C19-Pt1-Cl1 = 89.83(12),  
470 C19-Pt1-C12 = 90.83(16), C19-Pt1-N1 = 100.39(15), N1-Pt1-Cl1 = 86.89(9),  
471 N2-Pt1-Cl1 = 85.35(9), N2-Pt1-N1 = 79.72(12).

472 **Figure 2.** Eyring plot for the oxidative addition reaction of complex 1-Cl,Cl in the full set  
473 of solvents used in the study.

474 **Figure 3.** Activation enthalpy/entropy compensation plot for the full series of concerted  
475 oxidative addition C-X activation reactions indicated in Table 2. Numbering indicates the  
476 table entries of the data from the literature.

477 **Figure 4.**  $\Delta V^\ddagger/\Delta S^\ddagger$  correlation plot for the full series of concerted oxidative addition C-X  
478 activation reactions indicated in Table 2. Numbering indicates the table entries of the data  
479 from the literature.

480

481

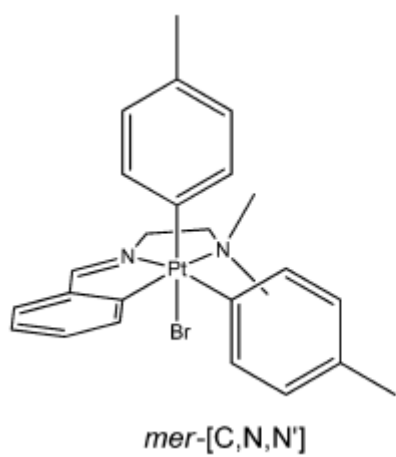
482

483

484



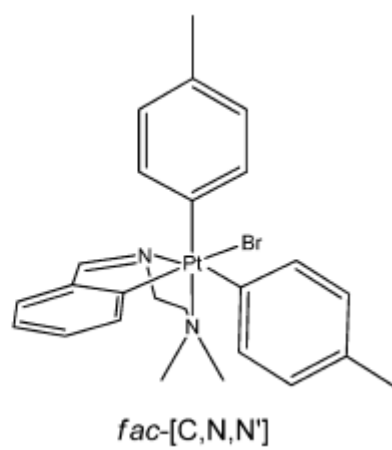
491 **Scheme 1.**



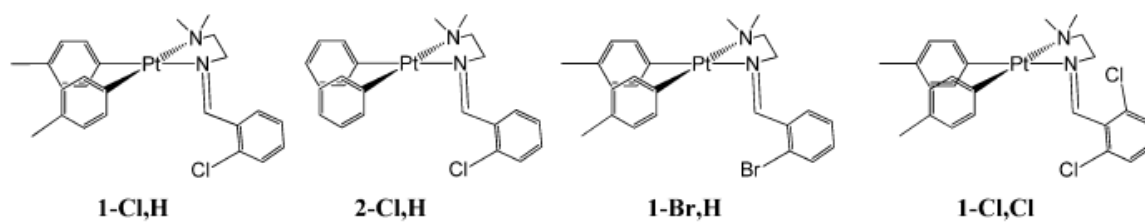
492

493

494



495 **Scheme 2.**



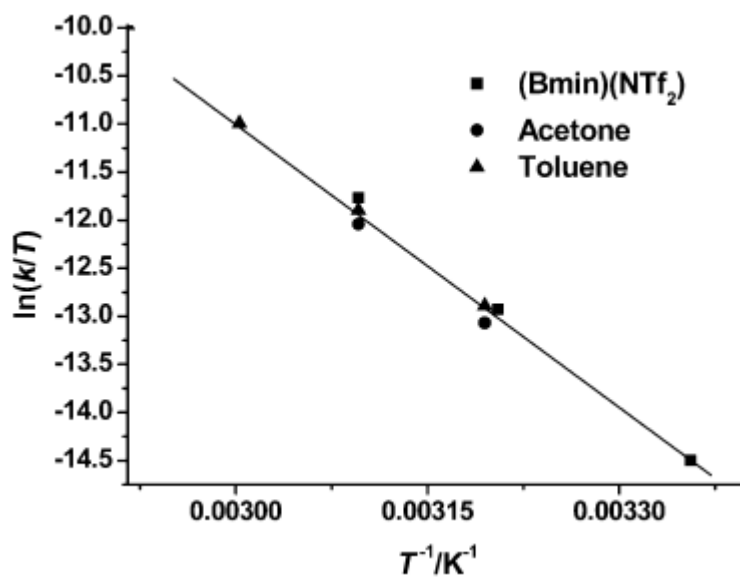
496

497

498

499 **Figure 2**

500



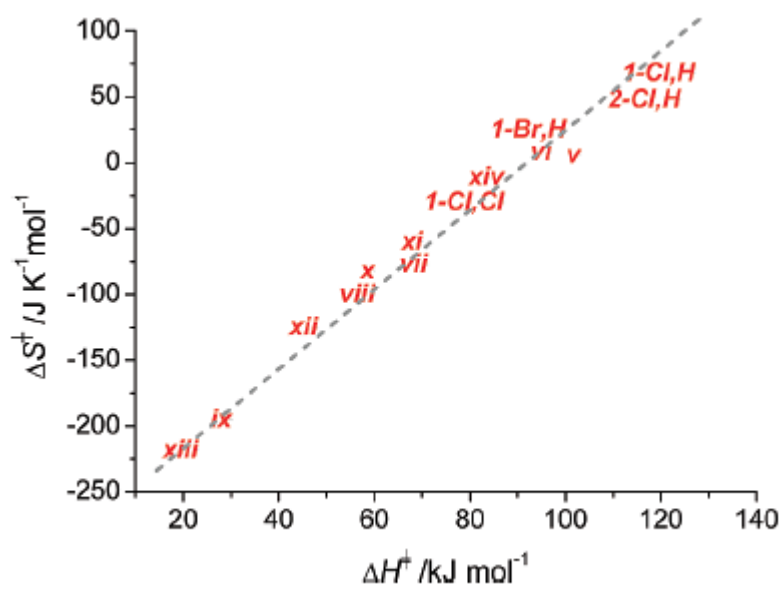
501

502

503

504 **Figure 3**

505



506

507

508

509

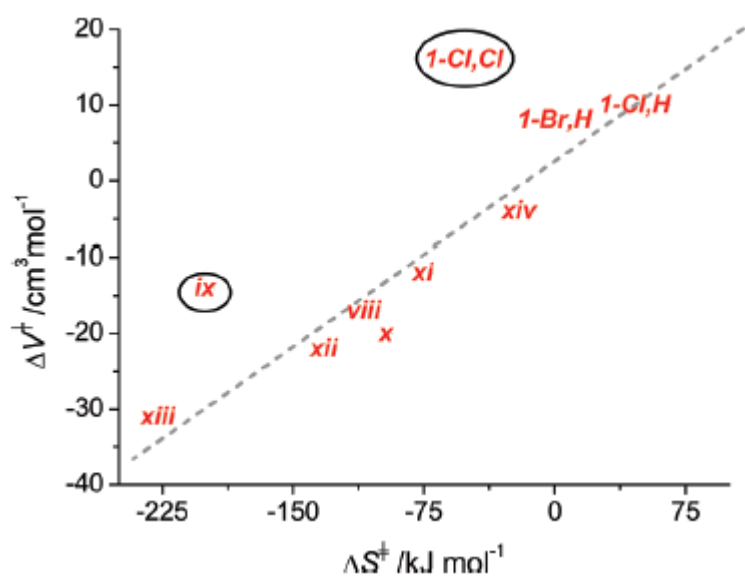
510

511

512

513

514 **Figure 4**

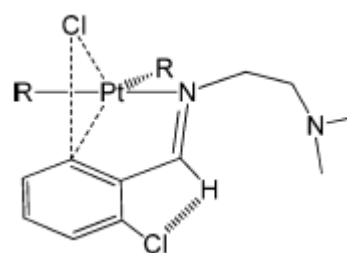


515

516

517

518 **Scheme 3**



519

520

521

522

523

524

525